

MEASUREMENTS OF THE PERFORMANCE OF A HELICOPTER  
SWEPT TIP ROTOR IN FLIGHT

by

M. J. Riley

Royal Aircraft Establishment, ENGLAND

ABSTRACT

Swept and rectangular planforms have been flight tested simultaneously on a single rotor. Surface pressure distributions have shown the swept tip to perform well on the retreating blade and in the highly loaded areas at the front and rear of the rotor disc as well as on the advancing blade. Blade dynamic response measurements have demonstrated the effectiveness of the chosen planform in controlling aerodynamic pitching moments and overall power measurements indicate a reduction of the power required by the swept tip rotor.

1 INTRODUCTION

The Royal Aircraft Establishment at Bedford, UK, in a collaborative research programme with ONERA and Aerospatiale in France, have conducted a series of flight tests to measure the surface pressure distributions on an experimental swept planform constructed on the tip of a Puma helicopter blade, Fig 1. The primary objective of the experiment was to provide a detailed description of the flowfield in the tip region. This was needed to guide the development of the prediction methods for the design of advanced swept tip shapes intended to delay the adverse effects of increasing tip Mach number on the advancing blade. Riley and Miller, Ref 1, at the Ninth European rotorcraft Forum, gave some preliminary comparisons between the measured and predicted chordwise pressure distributions in the advancing blade region. The measurements given in the paper demonstrated the effectiveness of sweep in alleviating the adverse high Mach number effects near the tip of the advancing blade, and confirmed the accuracy of the prediction methods used to calculate the flowfield in the tip region. Also of importance in assessing the contribution of swept tip planforms to overall rotor performance is their behaviour in the retreating blade area and in the highly loaded regions at the front and rear of the rotor disc. A further aspect of their performance concerns the aeroelastic response of the blade in view of the potential coupling introduced by the sweepback. This paper presents results from flight experiments which address these further aspects of swept tip performance; in addition some examples of measurements of the total rotor power requirement are included.

Reference 1 described the design of the swept tip and gave details of the pressure sensor installation on the experimental blades, and of the recording techniques used in flight. The flight tests were conducted essentially as a comparative experiment, since simultaneous measurements were made on the new swept tip and on an equivalent rectangular tip fitted to the opposite blade of the Puma helicopter. The diagram in Fig 2 indicates the chordlines fitted with pressure sensors on each of these blades. It was found that the helicopter could be flown satisfactorily with the swept and rectangular blades both fitted, or with four swept tip blades fitted, as in Fig 1. Indeed, full exploitation of the Puma as a test vehicle to provide

either the most demanding advancing or retreating blade conditions, required an extension to the normal operating speed range, reduced and increased rotor speed settings and an increase in the maximum permitted power input levels. All these were attainable with the experimental blades, within the permitted stress levels in the rotor system.

## 2 PERFORMANCE OF SWEEPED TIP IN BLADE STALL REGIONS

Sweepback is used on the blade tip to reduce the Mach number of the component of the flow normal to the local isobars and is a recognised method of reducing shock strength in the advancing blade region. Alternative approaches would be to use thin un-cambered blade sections in the tip region or limit the blade tip speed, constraints which conflict with the aerodynamic requirements in the retreating blade region. The introduction of sweep enables a balance to be struck which is more favourable to the retreating blade demands, and in addition the swept planform introduces new features to the aerodynamics of the flow in the high incidence conditions on the retreating blade. It is possible that the highly swept blade leading edge will generate a stable edge-vortex type of flow as on a delta winged aircraft at high incidence, and that this will not only maintain high lift levels but may also avoid the stall hysteresis which gives pitching moments leading to negative torsional damping beyond stall on an un-swept planform. A further distinguishing feature of the RAE swept tip geometry is the abrupt forward displacement of the leading edge line just inboard of 0.9 radius. It is anticipated that this 'notch' at the inboard extremity of the swept region will stabilise the leading edge vortex flow pattern and may thus help to prevent the spread of stall from regions further inboard on the blade. The flight measurements have been used to investigate these planform - dependent effects.

To assess the significance of these planform effects in influencing blade stall, flight test conditions at high speed and thrust were chosen to produce extensive blade stall on the Puma helicopter and measurements of the surface pressure distributions and accompanying blade dynamic response were made on both the swept and rectangular tip blades. Since straight flight conditions within the normal operating flight envelope for the Puma were not found to produce extensive stall in the blade tip regions, special clearance to operate beyond the normal limits was obtained. This was subject to continuous monitoring of oscillatory stress levels in the experimental blades and control system by telemetry to a ground station during each flight, allowing higher maximum flight speeds, and operation at reduced rotor speed. In addition, considerably higher power input levels were used subject to the direct monitoring of main rotor torque in place of the usual collective pitch limits specified for the Puma.

The flight measurements were used to assess the differences in the azimuthal extent of stall in the blade tip region on the swept and rectangular blade tips, and to make a detailed interpretation of the pressure distributions in the azimuth regions beyond the onset of separation, and of the forces and moments they produce.

A criteria to define the onset of separation near the leading edge can be taken as the point at which the local leading edge suction peak abruptly ceases to grow in the rising incidence gradient on the retreating blade. To establish how the sweep affects the azimuth position for the onset of separation in the tip region, it is helpful to consider the factors which underlie the main features of the loading pattern on the retreating blade. The measurements from the swept tip in Fig 3 show the sequence of rapid rises and

falls of both the leading edge suction peak and the local lift coefficient at the 0.95 radius position. These relate to the onset of separation, and also to the rapid changes of incidence that the blade encounters. The measurements indicate that the most significant incidence perturbations in the retreating blade area for this flight condition are attributable to the blade twisting and to the interaction with the vortex trailed from near the tip of the preceding blade which causes stall to spread towards the tip from inboard on the blade.

The development of the pattern of the retreating blade loadings is shown by tracing the progression of the azimuth position of the first peak in the leading edge suction at 0.95 radius relative to tip vortex and twist induced incidence perturbations for a range of increasing flight speeds (Fig 4). In this plot the position in azimuth of the incidence peak due to the first torsional mode of deformation is derived from the measurement of the blade pitch control load. The vortex crossing point, which is immediately preceded by its associated maximum upwash, is calculated using a simple undistorted wake representation of the vortex path - a method well substantiated by earlier flight test measurements at RAE. The overall pattern shows that throughout this speed range, the incidence peak due to twist precedes the wake disturbance and the separation onset occurs in the build-up of incidence towards this local maximum of blade twist. At the higher speeds, the phase of the torsion response advances to positions earlier in the azimuth, and the separation onset continues to precede it. These same trends are equally apparent in the measurements derived from both the swept and the rectangular tipped blades, and suggest that the blade twisting is the dominant parameter in fixing the azimuth location of separation onset, so that the sweep effect is only significant in so far as it modifies the torsional response of the blade, and not primarily in terms of its effect on the local aerodynamics of the tip section.

Turning now to the possibility of a stable leading edge vortex type of flow on the swept tip, measurements have been made of the chordwise pressure distributions on both the swept and rectangular tip planforms to study the differences in behaviour beyond the initial separation. Clearly the flowfield in the tip region is very time dependent, so that individual pressure distributions measured at a particular azimuth angle must be interpreted with care if planform effects are to be recognised during dynamic stall. Equally, the essentially three dimensional nature of the flow requires that the simultaneous measurements made for the four chordlines on the swept tip be studied together. An example of the upper surface pressure distribution measured on the rectangular tip in Fig 5 at an azimuth position corresponding to the maximum lift at 0.95 radius, shows how the separation, spreading from inboard on the blade, has caused a collapse of the suction peak at 0.89 radius, but has yet to reach the 0.95 and 0.98 radial stations, which continue to maintain a high lift level. Somewhat in contrast to these chordwise pressure distributions on the rectangular tip, are the measurements from the swept tip in Fig 6, at an azimuth angle where high lift levels are again reached, beyond the blade-vortex interaction at this radius. They are representative of the chordwise distributions where high lift is maintained after leading edge separation on the swept tip, and these upper surface pressure distributions at the 0.95 and 0.98 radius position suggest that a stable leading edge vortex has been established.

### 3 LOADINGS AT FRONT AND REAR OF ROTOR DISC

Since overall rotor performance depends on the blade tip behaviour at all azimuth angles, as well as in the specific advancing and retreating blade 'problem areas', it is important to establish that there are no significant performance penalties associated with sweep in the highly loaded areas near the front and rear of the rotor disc. Addition of the rotational and translational velocities of the blade results in a continuously varying velocity component normal to the leading edge as the blade rotates. For a region of azimuth near the front of the rotor disc, this component is larger for a swept tip than for a standard straight blade, since the sweepback effectively cancels the usual inclination of the flow to the local chordline. The changes in the Mach number of the flow normal to the leading edge at 0.95 radius are shown in Fig 7 for a high speed flight condition, comparing a straight blade with one swept back at an angle of 25 degrees. Clearly there is a significant reduction of the Mach number at the rear of the disc, but around the 180 degrees azimuth position there is a region of moderately high incidence and Mach number where the swept tip encounters a Mach number normal to the leading edge slightly higher than that for a normal straight blade. The chordwise pressure distributions enable us to assess the performance of the swept tip for this particular combination of incidence and Mach number.

A full analysis of the relative performance of the blade tips can be made by comparing shock strengths and the chordwise extent of the supercritical flow for the whole of these regions. Pressure distributions at 0.95 radius for azimuth angles where the lift coefficients are the same for each blade have been chosen as examples to illustrate the effect of sweep in these areas of the rotor disc, Fig 8. In the upper plot at 40 degrees azimuth the large low pressure area on the forward part of the rectangular blade section shows the extent of the supercritical flow area, terminating in a shock located quite far aft along the chordline. The swept tip has a more favourable pressure distribution indicative of the lower drag and smaller pitching moment expected of the lower Mach number. At the 160 degree azimuth position, where the Mach number of the component normal to the leading edge is higher for the swept tip, it is clear that there is no significant penalty in terms of shock strength or location, since the pressure distribution shapes are substantially the same for both tip shapes - demonstrating a satisfactory performance in both of these areas of the rotor disc.

### 4 BLADE DYNAMIC RESPONSE

On the RAE swept tip, the area distribution both forward and rearward of the blade torsional axis is intended to minimise the aeroelastic coupling due to the aerodynamic pitching moments generated in the tip area. Since the air-loads distribution varies considerably as the blade rotates, and indeed can not be established from theoretical calculations precisely, it is important to examine the effect on the blade torsional response of any residual aerodynamic moments which may be present. Similarly, the design intention was to minimise increments in dynamic pitching moments by the location of a counter-balance weight in the forward extension to the tip region, but there is inevitably an increase in tip weight and torsional inertia on the modified blades relative to the standard Puma blades. The flight measurements included flap bending moments at fourteen radial positions, and lag bending and torsion at four radial positions. Using these measurements, strain pattern analysis techniques can be used to derive the amplitudes of the blade deformations to compare with the predicted

deformations. Also measured in the flight tests were the blade pitch control link loads, and in Fig 9 two examples of the measured pitch link loads are plotted as they provide a convenient way to illustrate the changes to the blade dynamic twist.

For the response of the blade near the first torsional mode frequency, the restraining force at the root is directly related to the blade incidence excursion in the tip region arising from dynamic twist. At the low airspeed of 61 knots, this response, at about five times rotor speed, shows a small increase in amplitude for the swept blade, and it is seen to persist through the 90 degree azimuth advancing blade region. The small incidence changes associated with these pitch link loads, contribute to the pattern of the aerodynamic loadings on the advancing blade, as confirmed by pressure measurements<sup>1</sup> on the blade tips in this region of azimuth. They cause significant supercritical flow areas on the blade in the first quadrant and again in the second quadrant, rather than near the 90 degree azimuth position as might be expected. In the lower plot in Fig 9, at a higher airspeed, the oscillatory pitch link loads are now considerably higher for both the swept and rectangular tip shapes. Comparing the blades, it is clear that although the amplitude of the overall response is not significantly different the phasing of the waveform at the first torsion mode frequency is sufficiently modified to change the aerodynamic loadings in both the advancing and retreating blade regions, confirming that aeroelastic tailoring can be an important aspect of good swept tip rotor design.

Quite apart from these detailed considerations of optimised rotor loading distributions, it is important to demonstrate that the aerodynamic and dynamic de-coupling for which the planform and counterweight were basically designed does achieve the desired blade dynamic behaviour. The successful operation of the experimental rotor throughout, and beyond, the standard aircraft flight envelope has given ample confirmation that this has been achieved. The pitch link load measurements again provide an example, Fig 10, which shows the gradual increase of oscillatory load levels which is typical of both the standard rotor and the experimental blades. The small increase of both the swept and rectangular blade oscillatory levels was found to be acceptable within the design limitations imposed by the superposition of different experimental planforms on the structure of blades of an existing rotor dynamic system.

## 5 OVERALL ROTOR POWER MEASUREMENTS

The objective of these flight tests was to make a detailed survey of the flowfield in the tip region of the swept and rectangular tips. However, since the overall rotor performance changes due to these local aerodynamic improvements are of direct interest an attempt was made to quantify these overall improvements by measuring the main rotor power requirement directly, first for the standard rotor, and then for the rotor fitted with swept tips on all four blades. As is usual in comparative tests of this kind, the flight conditions were chosen to enable power comparisons to be made at the same rotor thrust coefficients, tip Mach numbers and advance ratios. The same reference blade areas were used in defining the thrust and power coefficients for both rotor configurations, but in addition several direct power comparisons were achieved by test flights at the same weight and air temperature. These confirmed that the comparisons of results in coefficient form as defined above were not misleading. It should be recognised of course that the configuration changes included not only the incorporation of sweepback near the tip, but small changes in blade area, radial distributions

of area and blade section in the swept tip region, all of which might be expected to lead to performance changes in their own right.

The hover measurements in Figure 11 show how there is relatively little change in power required for a wide range of rotor thrust coefficients, there being perhaps a small reduction in the power required by the swept tip rotor at the higher thrust levels. In the forward flight tests, power was measured for a range of values of rotor thrust coefficient and blade tip Mach numbers and, whereas it was found that at low thrust coefficients there were only small differences in power between the two configurations for a wide range of tip Mach numbers, progressively larger power reductions were noted for the swept tips as thrust coefficient was increased. This is demonstrated well by the measurements in Fig 12 where, at the highest speed, the power reduction measured is approximately 12% - a very encouraging result for the swept tip rotor, as expected from the improvements in blade aerodynamics measured in both the advancing and retreating areas of the rotor disc.

It is somewhat surprising that significant rotor performance improvements can be realised by the simple addition of experimental test pieces on the blades of an existing rotor system. More recent confirmation of the potential gains offered by swept tip planforms has been given by the BERP rotor<sup>3</sup> demonstrated on the Westland Lynx helicopter. The two planforms are compared in Fig 13 and it can be seen that some of the main features of the RAE planform are incorporated in the BERP tip, and have played a part in enabling this rotor to realise the substantial performance improvements demonstrated in its recent flight trials.

## 6 CONCLUSIONS

The flight experiment has proved to be a valuable source of measurements covering all aspects of the performance of the RAE swept tip in addition to the advancing blade flowfield studies which were the main objective of these tests.

On the retreating blade the pressure measurements have confirmed that the swept tip establishes a controlled leading edge separation giving favourable lift and moment characteristics at high incidence. At the front of the rotor disc where the inclination of the oncoming stream tends to cancel the applied sweepback, no combinations of incidence and Mach number have been revealed by the measurements which give unfavourable pressure distributions on the swept tip. The forward extension of the tip planform inboard of the swept back area has been demonstrated to balance the aerodynamic pitching moments, and the overall blade dynamic behaviour proved to be satisfactory.

In terms of overall rotor performance, the RAE swept tip rotor has a significantly reduced power requirement relative to the standard Puma rotor. It is rewarding to see the results of this research at the RAE have now been incorporated in an advanced rotor design<sup>3</sup>, in the form of the BERP rotor now being flown on the Lynx as a demonstrator for Westland helicopter rotor designs.

REFERENCES

1. M J Riley,  
Judith V Miller  
  
Pressure distributions on a helicopter swept tip from flight tests and from calculations.  
  
Proceedings of the 9th European Rotorcraft Forum, Garmisch-Partenkirchen September 1983.
2. A R Walker,  
D B Payen  
  
Experimental application of Strain Pattern Analysis (SPA) - wind tunnel and flight test results.  
  
Proceedings of the 12th European Rotorcraft Forum, Garmisch-Partenkirchen September 1986.
3. R E Hansford  
  
Rotor load correlation with the ASP blade. Proceedings of the 42nd American Helicopter Society Forum, Washington, DC June 1986.



Fig 1 RAE Puma with swept-back blade tips.

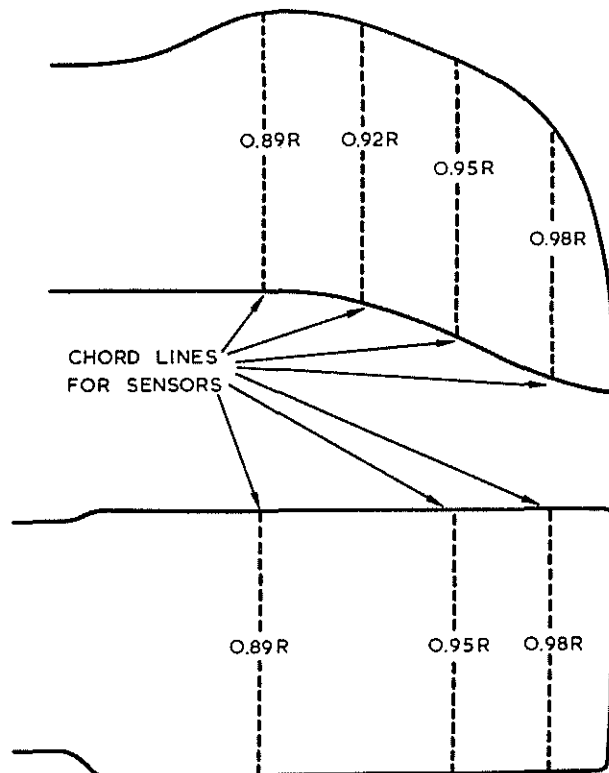


Fig 2 Planforms for swept and rectangular tips.

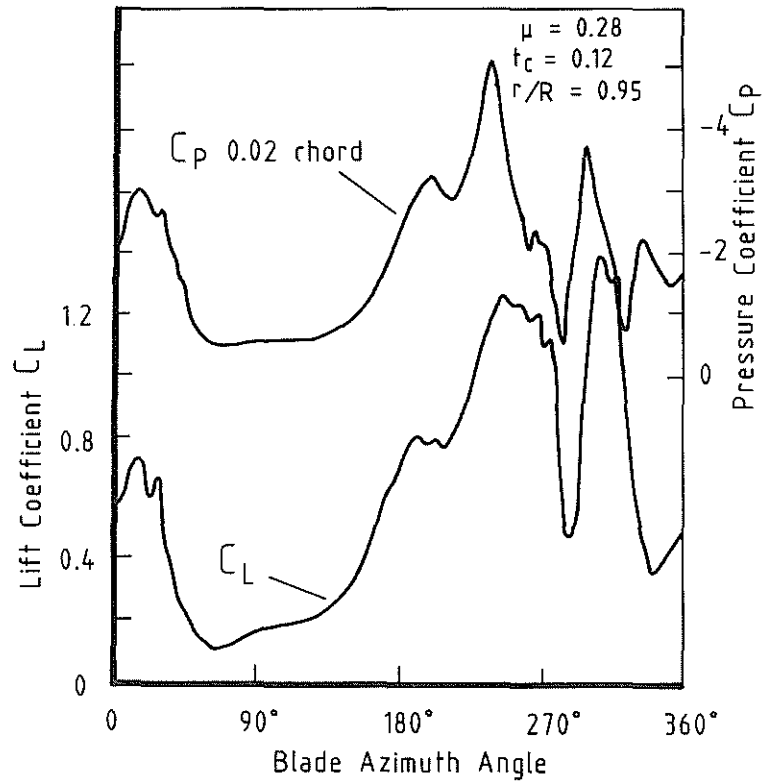


Fig 3 Rapid variations of loading on swept tip.

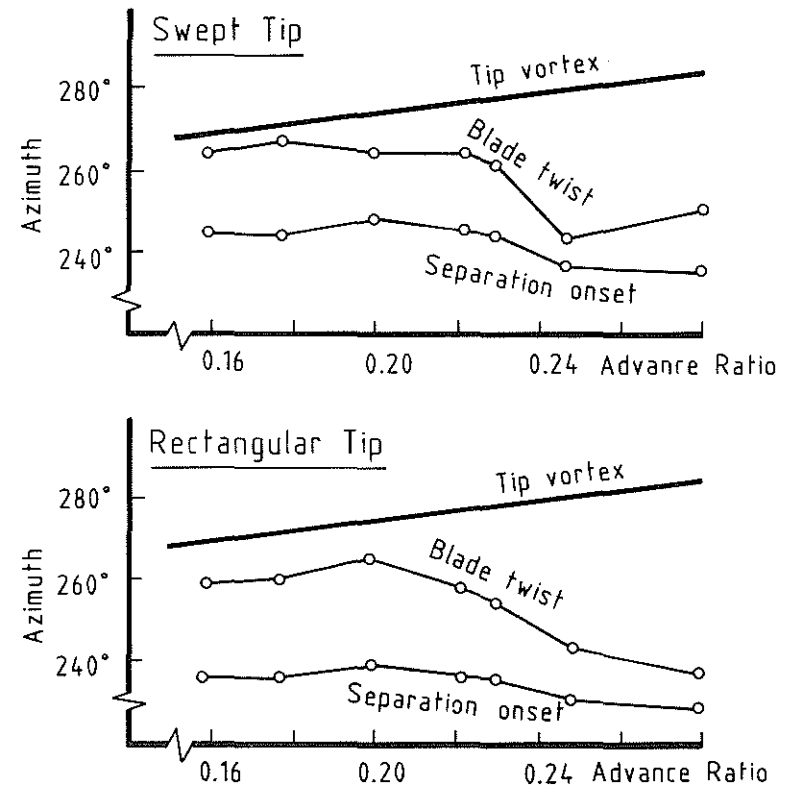


Fig 4 Separation onset position relative to local incidence perturbations.

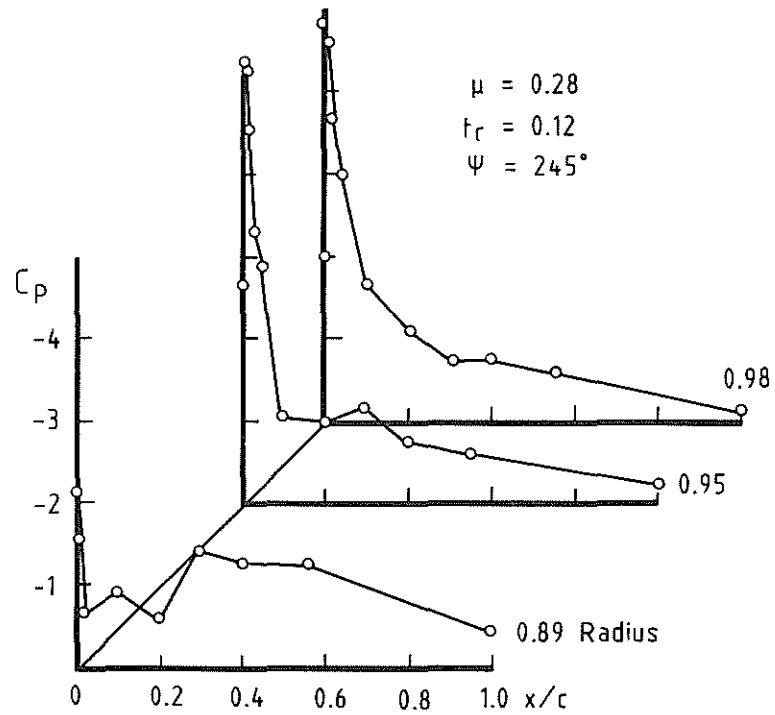


Fig 5 Surface pressures showing stall onset on rectangular tip.

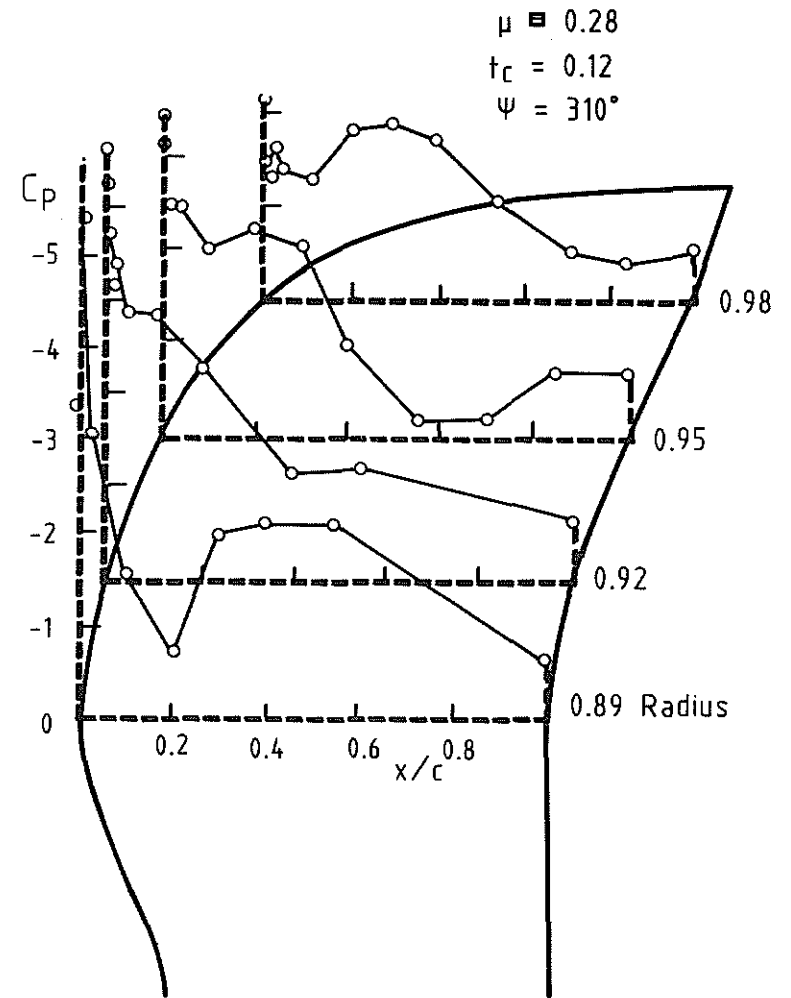


Fig 6 Stable leading edge separation on swept tip.

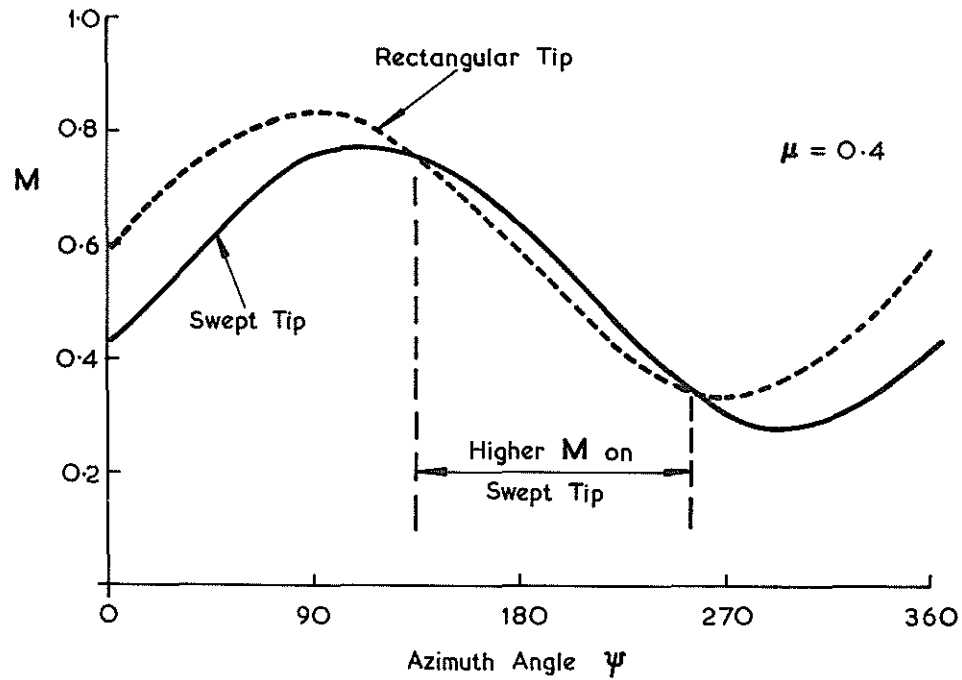


Fig 7 Blade Mach number normal to leading edge at 0.95 radius.

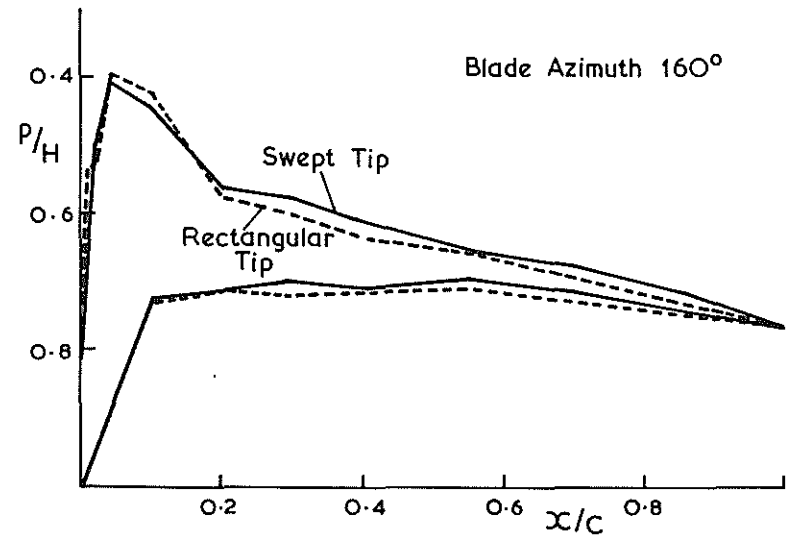
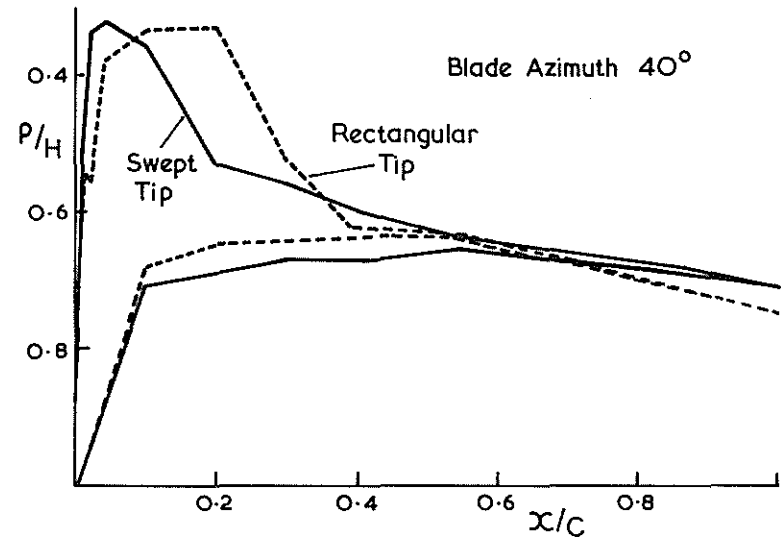
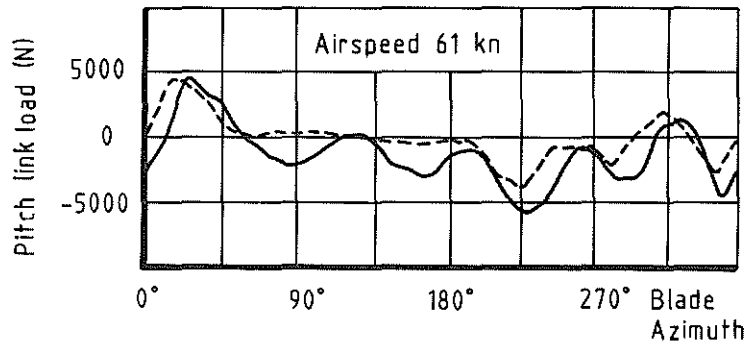


Fig 8 Pressure distributions near front and rear of rotor disc.



— Swept Tip  
 - - - Rectangular Tip

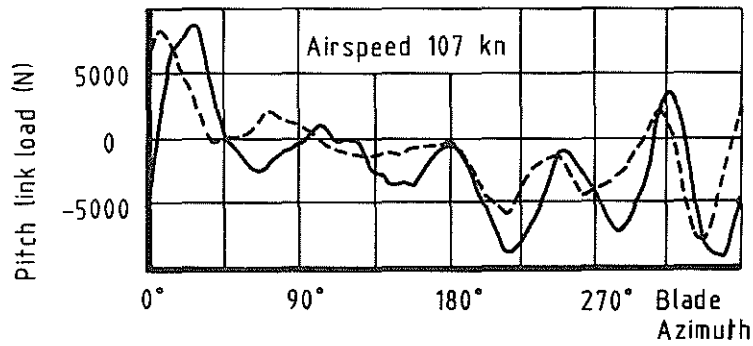


Fig 9 Pitch link loads showing blade dynamic twist.

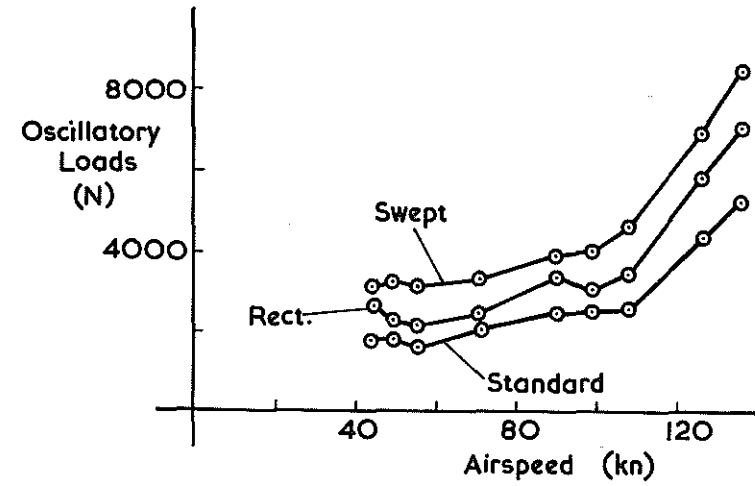


Fig 10 Control loads for swept and standard blades.

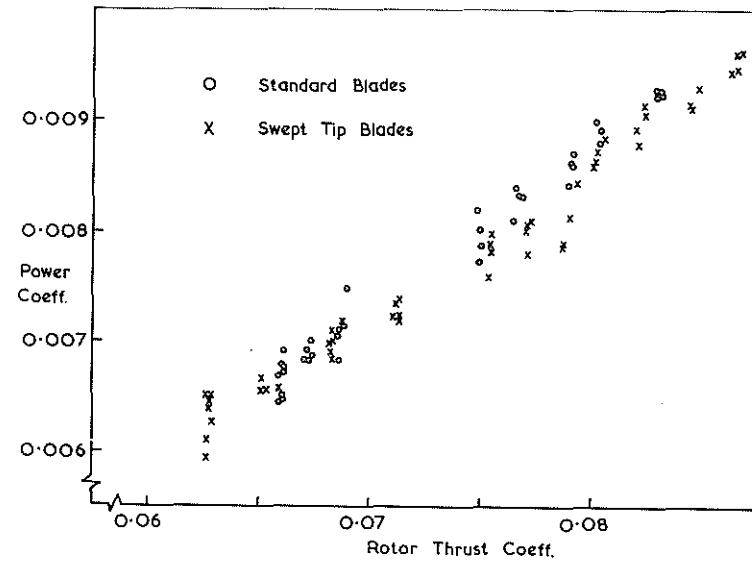


Fig 11 Hover power requirements for swept and standard rotors.

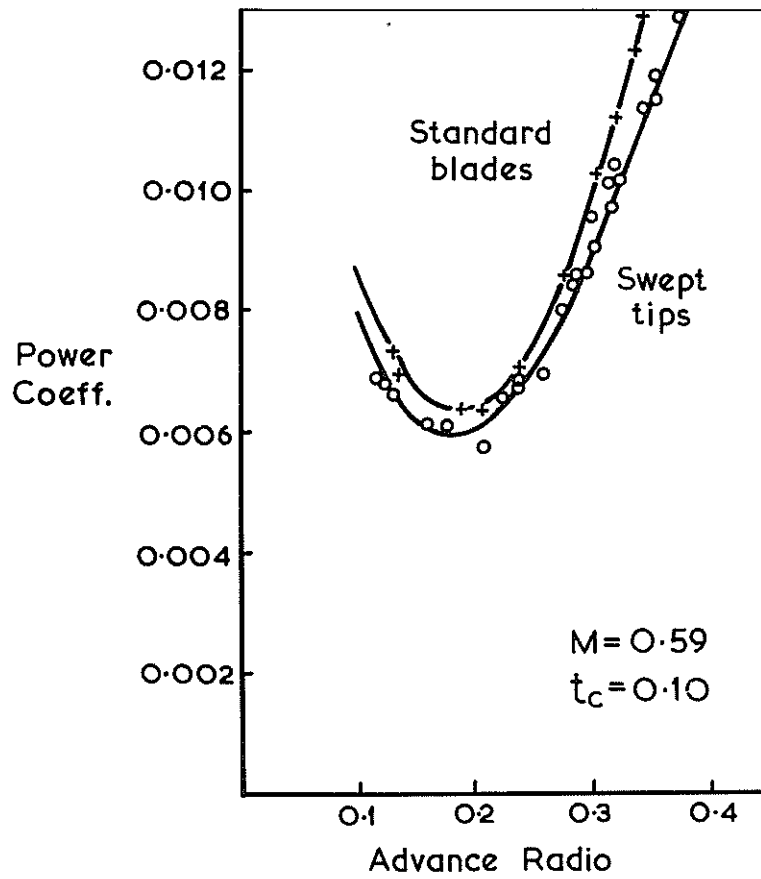


Fig 12 High speed power requirements for swept and standard rotors.

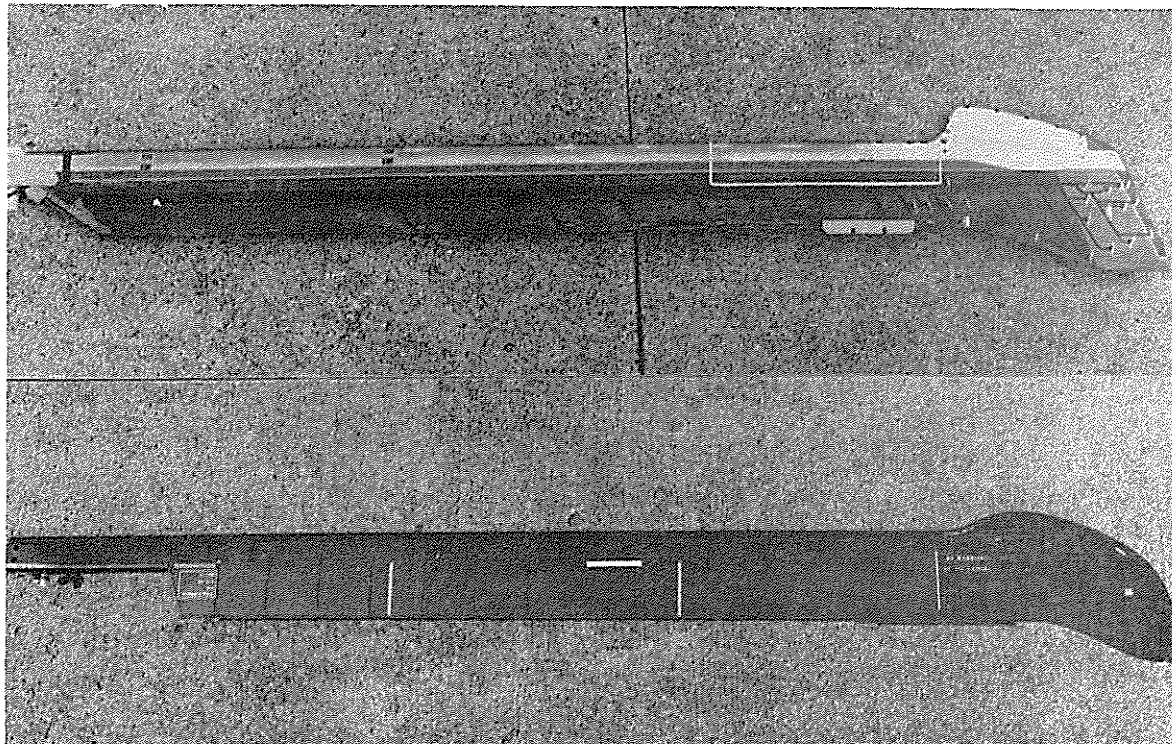


Fig 13 Planforms of Westland BERP blade and RAE Puma swept tip.